Earth and Planetary Science Letters 375 (2013) 303–311

Contents lists available at ScienceDirect

Earth and Planetary Science Letters

journal homepage: www.elsevier.com/locate/epsl

Repeated large Slow Slip Events at the southcentral Alaska subduction zone

Yuning Fu*, Jeffrey T. Freymueller

Geophysical Institute, University of Alaska Fairbanks, AK, USA

ARTICLE INFO

Article history:
Received 25 March 2013
Received in revised form
26 May 2013
Accepted 28 May 2013
Editor: P. Shearer
Available online 25 June 2013

Keywords:
Slow Slip Event
Alaska subduction zone
GPS
transient deformation

ABSTRACT

We identify and study an ongoing Slow Slip Event (SSE) in the southcentral Alaska subduction zone using GPS measurements. This is the second large SSE in this region since modern geodetic measurements became available in 1993. We divide the ongoing SSE into two phases according to their transient displacement time evolution; their slip distributions are similar to each other but slip rates are slightly different. This ongoing SSE occurs downdip of the main asperity that ruptured in the 1964 Alaska earthquake, on the same part of the subduction interface as the earlier 1998–2001 SSE. The average slip rate of this SSE is ~4–5 cm/yr, with a cumulative moment magnitude of *Mw* 7.5 (*Mw* 7.3 and *Mw* 7.1 For Phases I and II, respectively) through the end of 2012. The time and space dependence of the GPS displacements suggest that the slip area remained nearly the same during Phase I, while the slip rate increased with time. The SSEs occur on a transitional section of the subduction plate interface between the fully locked updip part and the freely slipping deeper part. During the 1964 earthquake, slip on the region of the SSE was much lower than slip in the updip region. Based on this observation and the repeated SSEs, we conclude that this part of the interface slips repeatedly in SSEs throughout the interseismic period and does not build up a large slip deficit to be released through large slip in earthquakes.

1. Introduction

Slow Slip Events (SSEs) have been observed and reported in many subduction zones, and their durations vary from days to years (Schwartz and Rokosky, 2007). SSEs in the Cascadia subduction zone last days to weeks with a typical duration of 3 weeks (Dragert et al., 2001), SSEs in Costa Rica last about 1 month (Jiang et al., 2012), a two-month SSE was reported by Ozawa et al. (2003) in central Japan, and SSEs in Mexico can be 6–7 months long (Kostoglodov et al., 2003). Hirose et al. (1999) identified an SSE with duration of about 1 yr in southwest Japan, and Wallace and Beavan (2006) studied a large SSE lasting one and a half years in New Zealand. The Tokai SSE (Ozawa et al., 2001; Yamamoto et al., 2005) lasted for several years.

Using Global Positioning System (GPS) measurements, Ohta et al. (2006) revealed an SSE in Upper Cook Inlet, in the southcentral Alaska Subduction Zone, during the period 1998–2001; its duration was much longer than most other SSEs. They found that the plate interface downdip of the 1964 earthquake rupture area slipped more than 10 cm within the SSE period, while the shallow part, the 1964 seismogenic zone, was fully locked during the SSE and therefore continued accumulating slip deficit for future earthquakes. Recently, Wei et al. (2012) identified another SSE in 2010–2011 in a comparable location in Lower Cook Inlet (Fig. 1).

In this paper, we systematically analyze the GPS timeseries around the southcentral Alaska subduction zone, and identify an ongoing SSE (as of the end of 2012) in the same area as the 1998–2001 SSE. We derive the GPS measured SSE surface displacements, determine the slow slip distribution on the subduction interface in space and time, and compare it with the 1998–2001 SSE.

2. An ongoing slow slip event

Forty-eight continuous GPS stations in southcentral Alaska are used for this study; 36 of them are part of the Plate Boundary Observatory (PBO) network, and another 12 stations belong to several other organizations (see the Auxiliary material for GPS station information). Fig. 1 shows the locations of GPS sites used in this study. We excluded GPS stations close to the Denali fault because of the potential for postseismic effects from the 2002 *Mw* 7.9 earthquake, and stations near volcanoes could be influenced by volcanic deformation. All the GPS data were processed in point positioning mode using GIPSY/OASIS II (version 5.0) software. We

* Corresponding author. Now at: Jet Propulsion Laboratory, California Institute of Technology, CA, USA. Tel.: +1 90 7750 8775.
E-mail address: yuning@gi.alaska.edu (Y. Fu).

0012-821X/$ - see front matter © 2013 Elsevier B.V. All rights reserved.
http://dx.doi.org/10.1016/j.epsl.2013.05.049

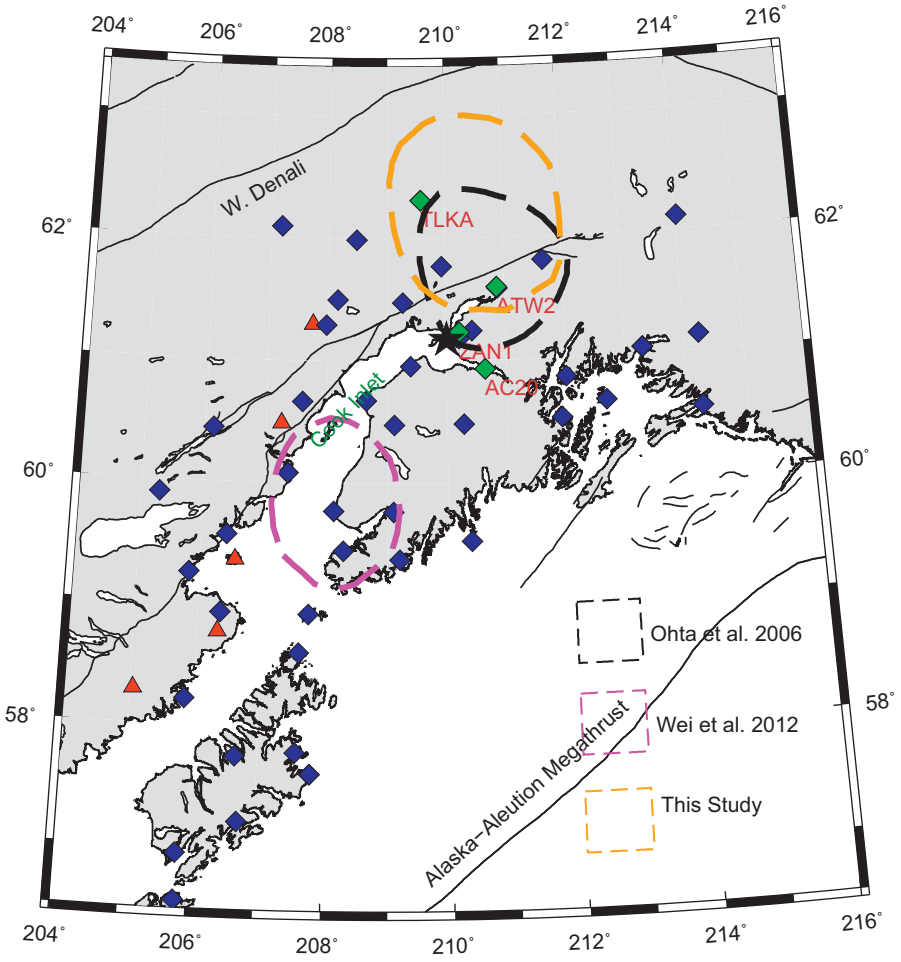

Fig. 1. Distribution of GPS stations used in this study. Diamonds are GPS stations; green diamonds are the stations whose timeseries are given in the auxiliary material. Red triangles are active volcanoes. The black star denotes the location of Anchorage. The three outlines indicate the previously identified SSEs of Ohta et al. (2006) and Wei et al. (2012), and the result of this study. (For interpretation of the references to color in this figure legend, the reader is referred to the web version of this article.)

adopted JPL's reanalyzed orbit and clock products (for the IGS repro2), and used the IGS05 absolute antenna phase models for corrections. Ocean Tidal Loading (OTL) effects were computed with ocean tide model TPXO7.0 and Greens functions modeled in CM (center of the mass of the whole Earth system) (Fu et al., 2012a). Individual daily solutions are then aligned with the ITRF2008 reference frame (ITRF2008.SNX). Refer to Fu and Freymueller (2012) for further data processing details.

Fig. 2 (top) shows a typical GPS timeseries for station ATW2 (see Fig. 1 for its location), a composite timeseries combining the PBO site ATW2 and a previous co-located continuous site ATWC using a measured survey tie. Due to the convergence between the Pacific and North American plates, the crust of southern Alaska moves landward (to the north) during interseismic periods (Freymueller et al., 2000, 2008), and GPS time series show this landward movement during 2001–2009 (Fig. 2, top).

However, GPS also observes movement opposite to the background linear trend of plate convergence during 1998–2001 and after 2009, because part of the plate interface undergoes slow slip. Those movements are in the same direction as the ground displacements caused by subduction zone earthquakes like the 1964 Prince William Sound earthquake (Cohen and Freymueller, 2004), but occur much more slowly.

In order to derive the SSE surface displacements from GPS timeseries, we analyze the GPS time series after the year 2003. We fit the steady deformation period with linear and seasonal (annual plus semiannual) terms, and the SSE period with linear, seasonal and a logarithmic relaxation term. We tried both logarithmic and exponential relaxation terms, and found that both can fit GPS timeseries equally well. Fig. 3 shows an example of fitted time series for both logarithmic and exponential functions. The seasonal effects in parts of southern Alaska are significant because of seasonal snow loading (Fu et al., 2012b), and that effect cannot be ignored. We adopt a grid search method to find the SSE start time that best fits both the GPS north and vertical components. We identify a starting time at the end of 2008 (2008.96) that minimizes the misfit between the measurements and the modeled time series. Fig. 3 gives an example for the north component of site ATW2 and its fitted timeseries showing steady deformation and the SSE displacement.

Here we define the SSE displacement as the position differences between the modeled steady movement and the actual observation (Fig. 3). During the earlier phase of this SSE, the GPS timeseries is more curved than the later phase; the later part shows linear motion, but at a different rate than the steady period. This suggests that the SSE displacement rate and/or slip area was growing with time in the earlier phase, while both are constant in the later phase. Therefore, we divided the whole event into two phases, Phase I (2008.96–2011.70) and Phase II (2011.70–2012.87), and investigate them separately. We then evaluate how slip in this SSE evolves with time.

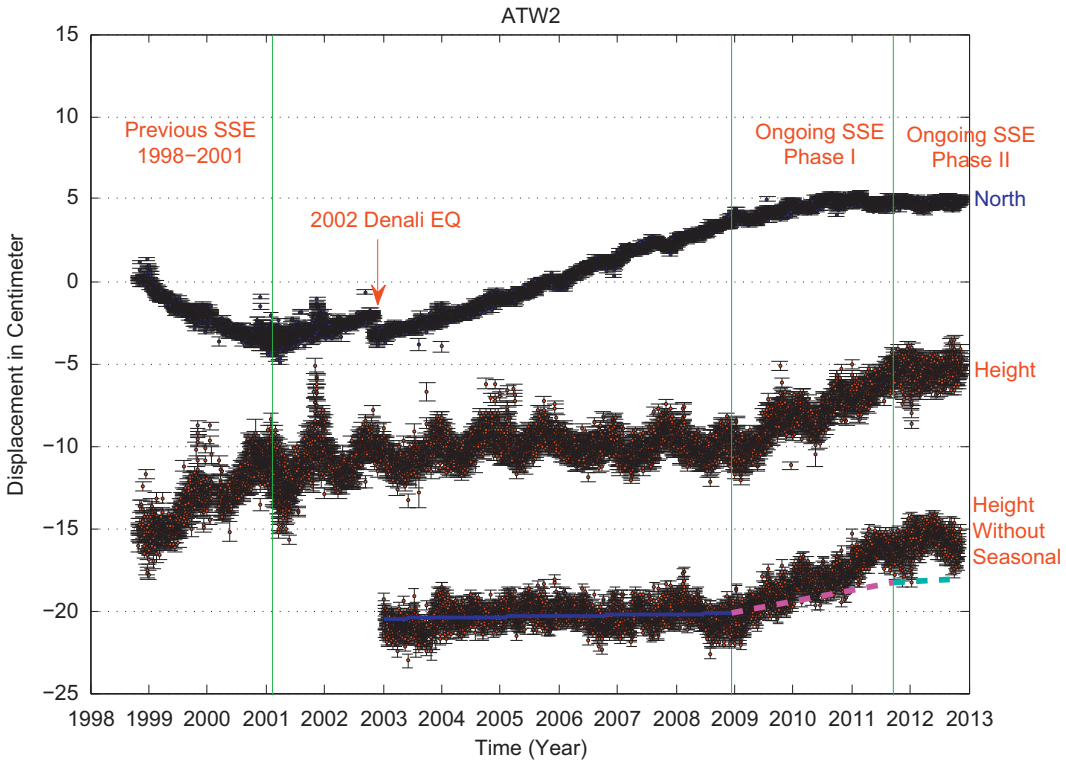

Fig. 2. A typical GPS timeseries showing the SSE. This is a composite time series combining the current PBO site ATW2 with a previous co-located continuous site ATWC. The top two time series are the north and height components relative to the stable North American plate (Argus et al., 2010). The bottom time series is the vertical position with seasonal effects removed using a GRACE-based model (Fu et al., 2012b). The predicted transient displacements from our model are added to the vertical velocity from the steady period; different colors indicate the two phases of the SSE. (For interpretation of the references to color in this figure legend, the reader is referred to the web version of this article.)

3. Slip model for the ongoing SSE

To investigate the SSE slip pattern, we employ a damped least squares inversion strategy to estimate the optimal slip distribution on the subduction interface. The Green's functions are based on a half-space elastic dislocation model (Okada, 1985). The details of this procedure were provided by Hreinsdóttir et al. (2006). We adopt the Slab 1.0 model (Hayes et al., 2012) for the geometry of the southern Alaska subduction interface. We use two curved fault groups to simulate the lateral geometric variation in the Slab 1.0 model (Fig. 4). The coseismic rupture area of the 1964 Prince William Sound earthquake is also highlighted with blue dashed lines in Fig. 4.

Fig. 5 shows the inversion results for both Phases I and II. The slip locations for both phases are the same, downdip of the Prince William Sound asperity of the 1964 rupture at 50–90 km depth, north of Anchorage. The cumulative moment magnitudes are *Mw* 7.3 and *Mw* 7.1 for Phases I and II, respectively; and *Mw* 7.5 for the whole event through late 2012 (2012.87), assuming a shear modulus of 30 GPa. Although the slip amplitudes are different between the two phases because the duration times differ, the average slip rates for each phase are close to each other, ~4–5 cm/yr. The slip rate distributions are very similar in both phases for the main part of the SSE, downdip of the 1964 rupture zone. The model for Phase II includes some slip to the south-southwest of this main patch, beneath the Kenai Peninsula. That slip roughly follows the downdip edge of the locked zone as estimated by Suito and Freymueller (2009).

We also did a slip deficit ("back-slip") inversion for the steady time period (2003–2008.96), and compared it with the Ohta et al. (2006) model. We first removed the effects of postseismic viscoelastic relaxation due to the 1964 Alaska earthquake using the model of Suito and Freymueller (2009). We find similar results to Ohta et al. (2006) in that the slip deficit reaches its maximum in the shallow part (depth < 40 km) of the plate interface (see the Auxiliary material), and the 1964 Alaska earthquake rupture zone (the shallow part of the interface) remains locked during both the steady period and the SSE period (Figs. 5 and 6, Auxiliary Fig. 2). During the steady time period the region of slow slip builds up a significant slip deficit, and there is no indication of any forward slip during the steady period within the area of SSE (Figs. 5 and 6). Thus, the SSE slip area behaves very differently from the shallow part of the interface, being locked or partially locked between SSEs and slipping during SSEs.

The average slip rate in Phase I is slightly smaller (by ~20%) than that of Phase II. The acceleration in the GPS time series during Phase I indicates the slip rate was variable in time, so what we estimate is actually an average rate. The slip rate of Phase II is essentially constant. All of the stations can be fit with the same time history (same logarithmic or exponential relaxation time) during Phase I (Fig. 7), so the acceleration seen in the Phase I period indicates that the slip rate in the SSE was increasing with time (over nearly the same slip area) until it reached a steady state in Phase II. Fig. 7 shows the GPS time series with the steady deformation rate subtracted, then normalized by the total Phase I displacement. All sites follow the same pattern, which confirms that the slip rate was increasing with time, while the slip area did not change substantially. If the slip area had increased with time, some stations would have shown a different time history than the others. Ohta et al. (2006) could not resolve variations in the slip rate for the earlier SSE in southcentral Alaska because most of their stations were surveyed in campaign mode; they could not constrain the onset time well either.

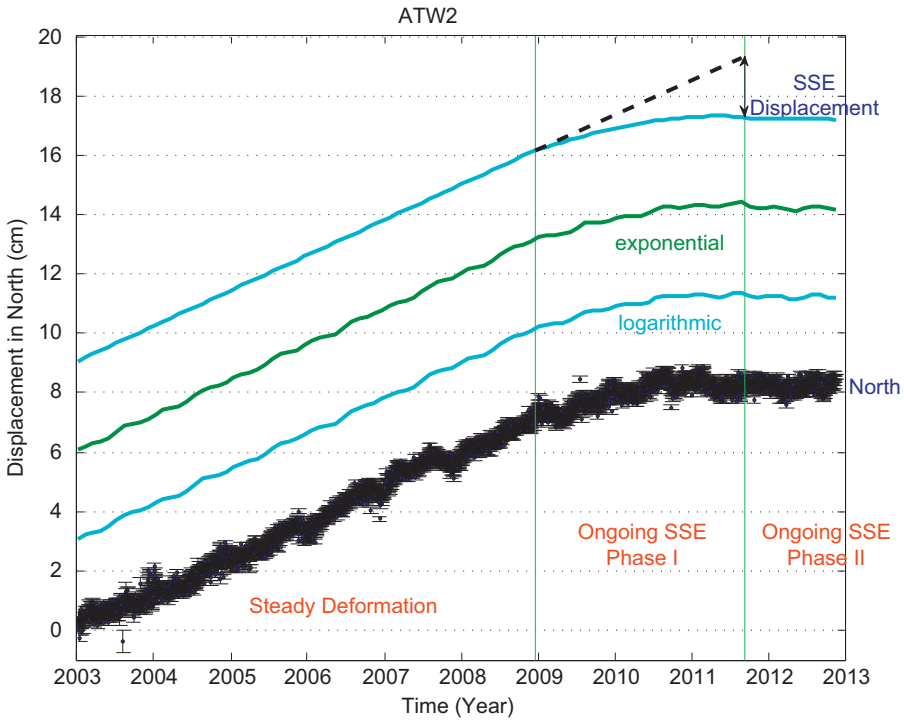

Fig. 3. The strategy used to extract the SSE displacement. We separate the whole SSE into two phases based on the deformation pattern. The SSE displacement rate grows with time during Phase I, but is constant during Phase II. An example for GPS station ATW2 is shown here, and more examples are provided in the auxiliary material. The fitted GPS time series with exponential and logarithmic relaxation (and seasonal) terms are also shown individually.

The location of slip in this ongoing SSE is nearly the same as that of the earlier 1998–2001 SSE (black dashed line) (Ohta et al., 2006); see Fig. 6. The differences in estimated SSE area may be due in part to the different plate interface models assumed in the two studies. After the 1998–2001 SSE, there was ~8 yr (~2001 to ~2009) of steady deformation before this section on the plate interface began slipping again and releasing the accumulated shear strain. The inverted SSE slip orientation varies from S10°E to S35°E with an average ~S20°E, similar to the convergence direction between the Pacific and North American plates. This would also be the expected coseismic rupture direction for a large earthquake in southern central Alaska subduction zone.

Wei et al. (2012) identified another SSE that took place beneath Lower Cook Inlet during 2010 and 2011 to the southwest of the SSE we model here (Fig. 1). Because they used data only up to 2011, during the growth of the SSE during Phase I, they did not identify the event we describe here, which is now substantially larger than the event they modeled. We also included data from additional continuous GPS sites from other sources, in addition to the PBO, which improves the ability of the network to detect and model events. Although the two events overlapped in time, there is a significant spatial gap between them and there does not appear to have been any slow slip in the gap between them.

4. Discussion

Two large SSEs have taken place in Upper Cook Inlet since GPS measurements became available for this region in 1993. The two events cover nearly the same area, which accumulated slip deficit before 1998 and during the time between the events. The SSE slip area did not have significant slip in 1964 (Suito and Freymueller, 2009), compared to the large slip in the main part of the rupture area. Savage (1983) proposed a simple model for the interseismic period of the subduction earthquake cycle, in which the upper part of the plate interface is locked and lower part is freely creeping. An improved model includes a transitional section between locking and slipping parts (Wang et al., 2003). SSEs occur repeatedly in this transition zone, therefore behaving as a buffer region to transfer and release strain and stress with time.

We can assess the slip budget for this section of the interface using the slip deficit distribution from the steady period (see Auxiliary material) and the slip distribution over the ongoing SSE (Fig. 5) and the previous event (Ohta et al., 2006). Averaged over the whole ongoing event, the peak slip rate of this ongoing SSE is ~4 cm/yr, decreasing to 1–2 cm/yr at greater depth. The total slip deficit over the ~8 yr steady period between events was 30–40 cm at shallower depth and ~10 cm at greater depth. Thus slip in the SSE has accounted for roughly a decade of the interseismic slip deficit over the SSE area, so this ongoing event has released most or all of the strain that accumulated during the steady period (~2001 to ~2009) between the two SSEs.

Combined with the earlier study of Ohta et al. (2006), our results suggest that the transitional region downdip of the 1964 Prince William Sound asperity slips repeatedly in large slow slip events. During 20 years that high precision geodetic data have been available, this part of the plate interface has accumulated very little net slip deficit, because slip in the two SSEs has roughly balanced the slip deficit during the inter-event periods. In contrast, the region updip of the two SSEs has remained fully locked since at least the beginning of the GPS data record in the area (1993), accumulating >1 m of slip deficit over that time, and corresponds to the 1964 coseismic rupture zone (Freymueller et al., 2008; Suito and Freymueller, 2009). Given that slip in 1964 in the area of the SSE was much smaller than slip in the shallower updip part of the interface (Suito and Freymueller, 2009), we conclude that last 20 years are representative of the interseismic period, and that most of the slip on this part of the interface occurs in slow slip events and probably not in large earthquakes.

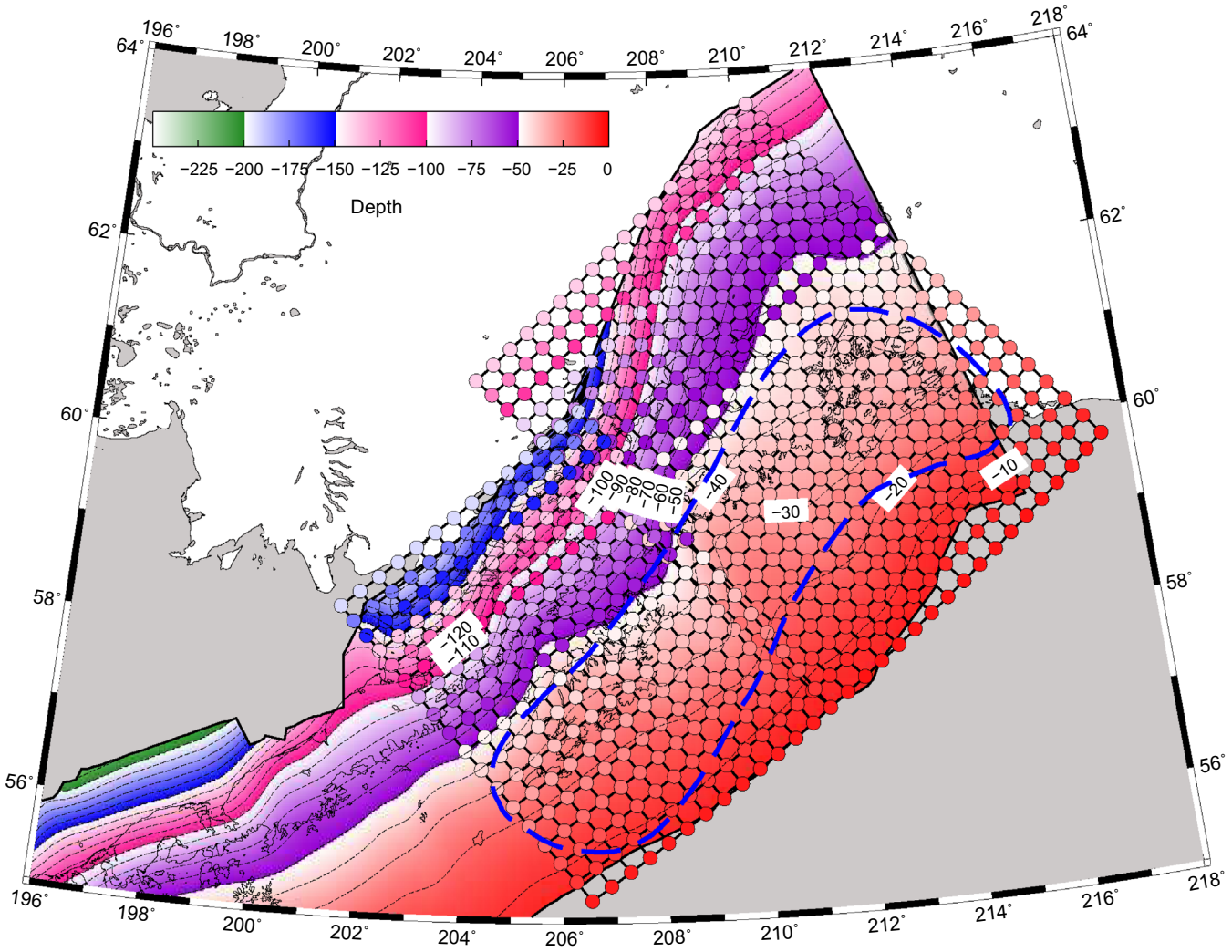

Fig. 4. Geometry of the subducting plate from Slab 1.0 (Hayes et al., 2012) for the southcentral Alaska subduction zone. The blue dashed line highlights the rupture area of the 1964 Alaska earthquake (Cohen and Freymueller, 2004). (For interpretation of the references to color in this figure legend, the reader is referred to the web version of this article.)

There was also significant afterslip on at least the shallow part of the SSE area in the first decade or two after the earthquake (Brown et al., 1977; Cohen and Freymueller, 2004; Suito and Freymueller, 2009).

Our results indicate this ongoing SSE is occurring at 50–90 km depth, which is deeper than SSEs of other subduction zones. Fig. 8 compares SSE depths at different subduction zones, and the depths of the large SSEs in Alaska do seem to extend to greater depth than at other subduction zones. We also used a synthetic inversion test to assess the resolution of our estimated slip distribution at the downdip end of the SSE. We computed displacements at the GPS sites for a synthetic slip model with uniform slip (dip slip only), and then inverted the synthetic data for the slip distribution. The estimated slip at the downdip end of the slip patch is smeared over at least one additional row of subfaults (see Fig. 3 of the Auxiliary material), although except for smearing at the edges of the slip patch the estimated slip distribution is very close to the input. If we picked the downdip end of the SSE area from the inverted synthetic model, we would estimate a depth 10–30 km deeper than the input model, depending on the local dip of the slab. This indicates that true maximum depth of slip in the SSE is probably shallower than 90 km.

Our estimated SSE region overlaps with and is nearly the same as the earlier 1998–2001 event, suggesting that the likely involved slip over the same part of the interface. The estimated depths of slip are different because the new Slab 1.0 model (Hayes et al., 2012) is deeper than the geometric model assumed by Ohta et al. (2006) for the SSE region. If Slab 1.0 is correct, then the depth of the 1998–2001 SSEs was probably deeper than Ohta et al.'s (2006) assessment of 25–45 km, and can reach 60–70 km. The 2010–2011 event also reached 70–80 km depth (see Fig. 1 of Wei et al., 2012). So the SSEs in the southcentral Alaska subduction zone extend to greater depth than SSEs at most of other subduction zones.

Slow slip events are usually accompanied by low frequency nonvolcanic tremor or increased seismic activities (Rogers and Dragert, 2003). Nonvolcanic tremor had been identified in southcentral Alaska within 1998 and 2001 during the previous large SSE (Peterson and Christensen, 2009). Wei et al. (2012) reported a small but still detectable seismicity increase around the 2010–2011 Lower Cook Inlet SSE, but no investigations have focused on the Anchorage area yet.

The GPS vertical component for SSE studies may be "contaminated" by the ground seasonal oscillations (most significant in height) caused by seasonal hydrological loading. The NASA and

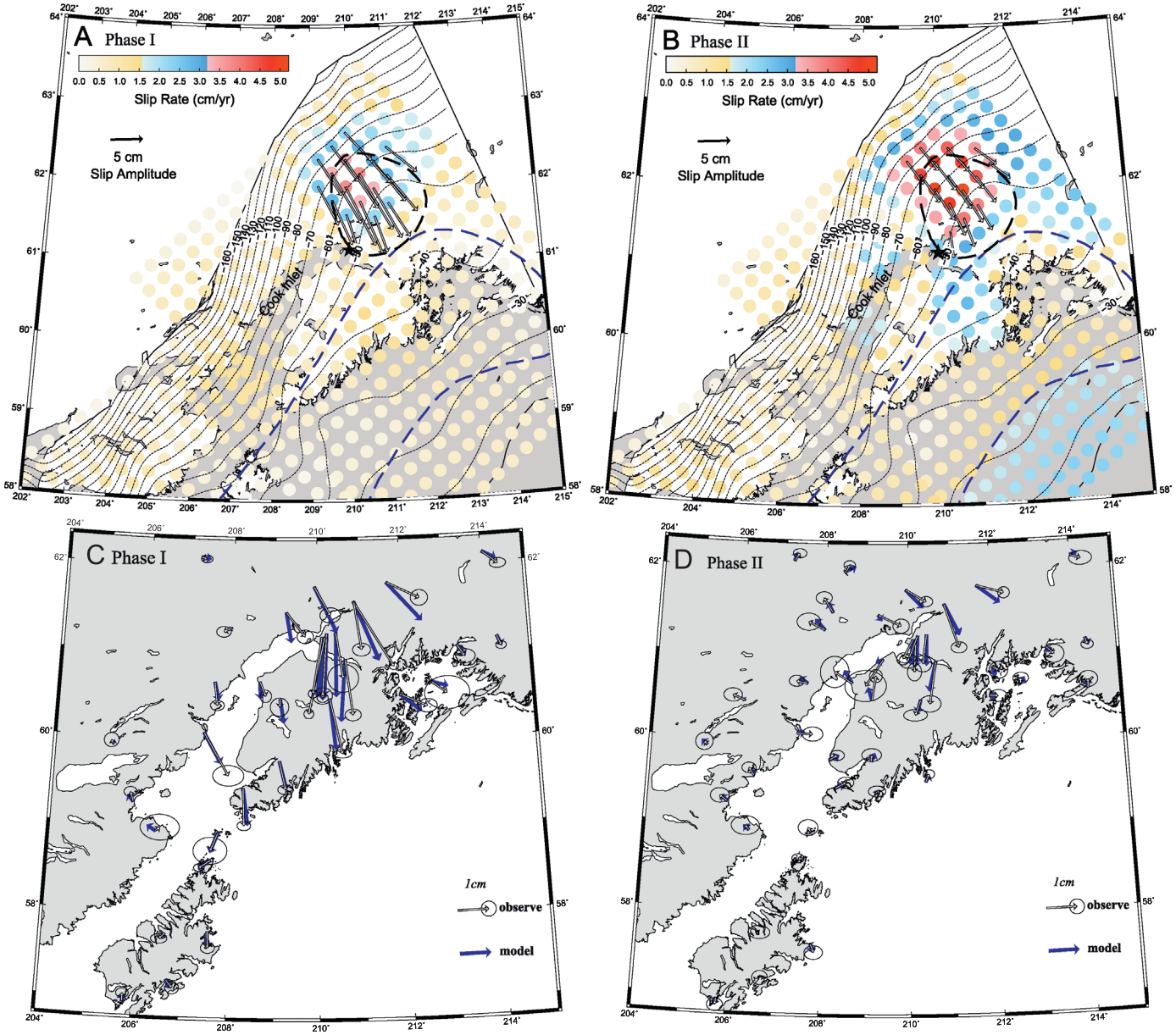

Fig. 5. Top: inverted slip distribution on the subduction slab for Phase I (A) and Phase II (B). The colors on the faults represent the slip rate. For comparison, the slip vectors (displacements, in cm) are also indicated. The blue dashed line highlights the rupture area of the 1964 Alaska earthquake. The black dashed lines show the locations of the previous 1998–2001 SSE (Ohta et al.). Bottom: Comparison between GPS measured SSE surface displacements and modeled results for both Phase I (C) and Phase II (D). (For interpretation of the references to color in this figure legend, the reader is referred to the web version of this article.)

DLR joint mission, Gravity Recovery and Climate Experiment (GRACE), is capable of quantifying the seasonal ground surface mass variation, and therefore may be used to model its resulting seasonal loading deformation. GPS observed and GRACE modeled vertical seasonal deformations are highly correlated across southern Alaska, indicating that snow loading is the dominant component to the seasonal deformation there (Fu et al., 2012b). The bottom of Fig. 2 shows the vertical position time series with the GRACE seasonal model removed, and the predicted transient displacement from our model added to the vertical velocity from the steady period. Our SSE model can explain roughly half (~50%) of the vertical displacements measured by GPS. The discrepancy requires further study; but removing the seasonal effect using a GRACE-based model is a promising way to make the vertical component more useful for these studies.

5. Conclusions

GPS measurements reveal a slow slip event in Upper Cook Inlet in the southcentral Alaska subduction zone since the end of 2008. This ongoing SSE is occurring downdip of the 1964 Alaska earthquake rupture zone. It started ~8 yr after the previous SSE in the same region, and already has reached a cumulative moment magnitude of *Mw* 7.5 as of the end of 2012. This SSE and the 1998–2001 event are located in a transitional (or buffer) region connecting the shallow seismogenic zone and deeper free slipping zone, and therefore is important for stress transfer between the seismogenic zone and mantle wedge in the subduction zone. This part of the interface accumulated slip deficit between SSEs, but the slip in SSEs roughly balances the slip deficit in the periods between events. In contrast, the shallower part of the interface

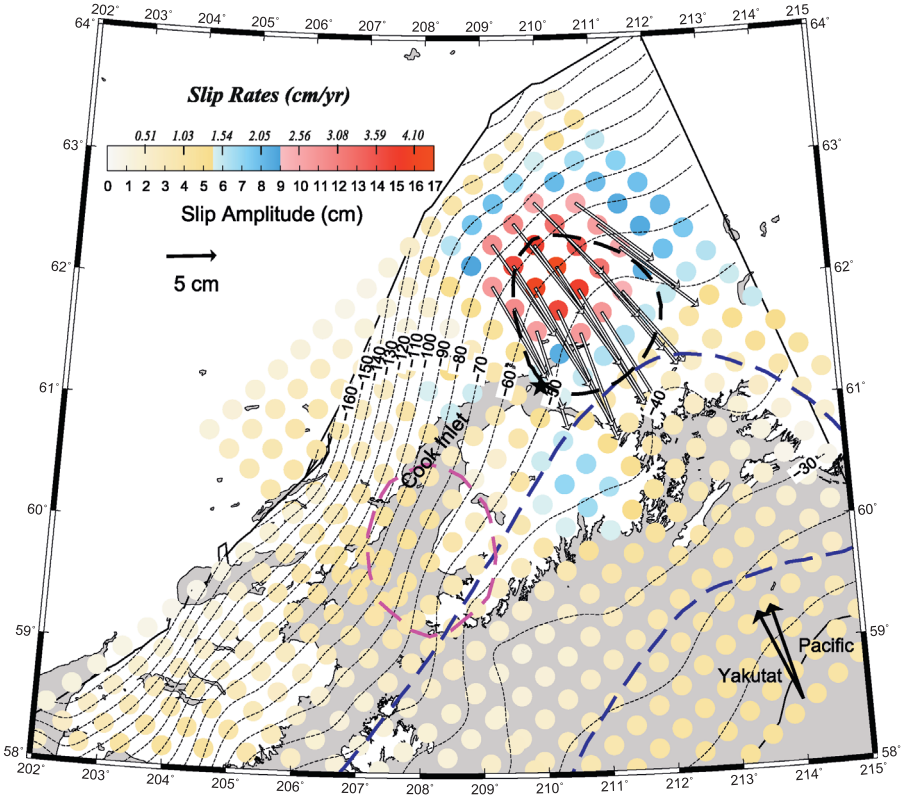

Fig. 6. Slip distribution for the whole event through the end of 2012. The black star indicates the location of Anchorage. The dashed lines show the locations of the previous 1998–2001 SSE in black (Ohta et al. (2006)), and the 2010–2011 event in magenta (Wei et al., 2012). The blue dashed line highlights the rupture area of the Alaska 1964 earthquake. (For interpretation of the references to color in this figure legend, the reader is referred to the web version of this article.)

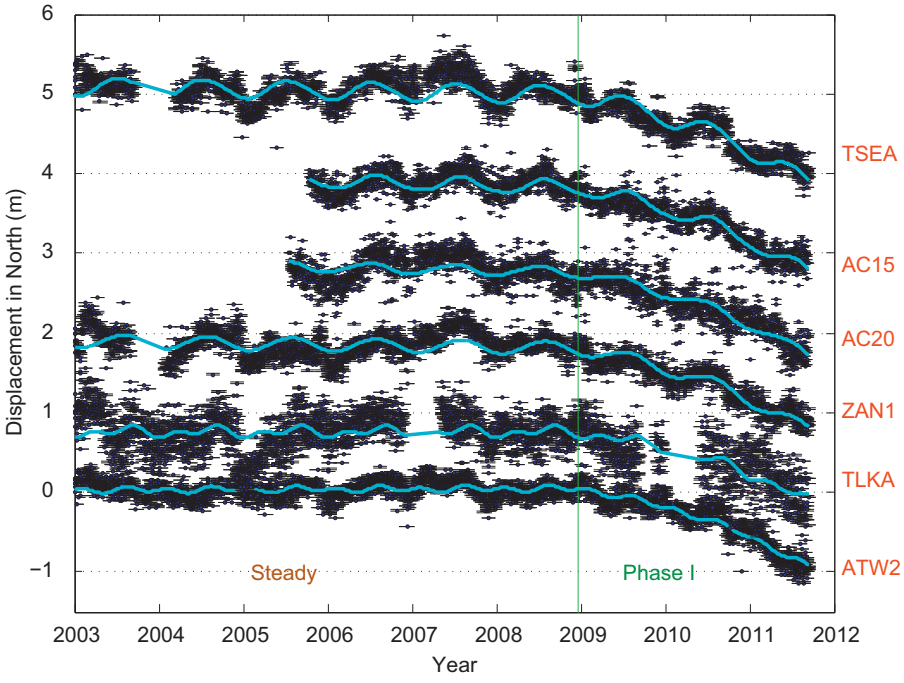

Fig. 7. GPS time series for several representative sites for Phase I with the steady deformation rate subtracted, normalized by the total Phase I displacement. All GPS time series follow the same pattern during Phase I, which indicates that the slip area remained constant during Phase I but the slip rate increased with time.

has accumulated a slip deficit of >1 m over the 20 yr period of modern geodetic observations. While the shallower part of the interface, immediately updip of the SSEs, had ~20 m or more of slip in 1964, the area of the SSEs did not experience significant slip in 1964. It is likely that most slip on this part of the interface occurs in slow slip events, or in afterslip after 1964-type events.

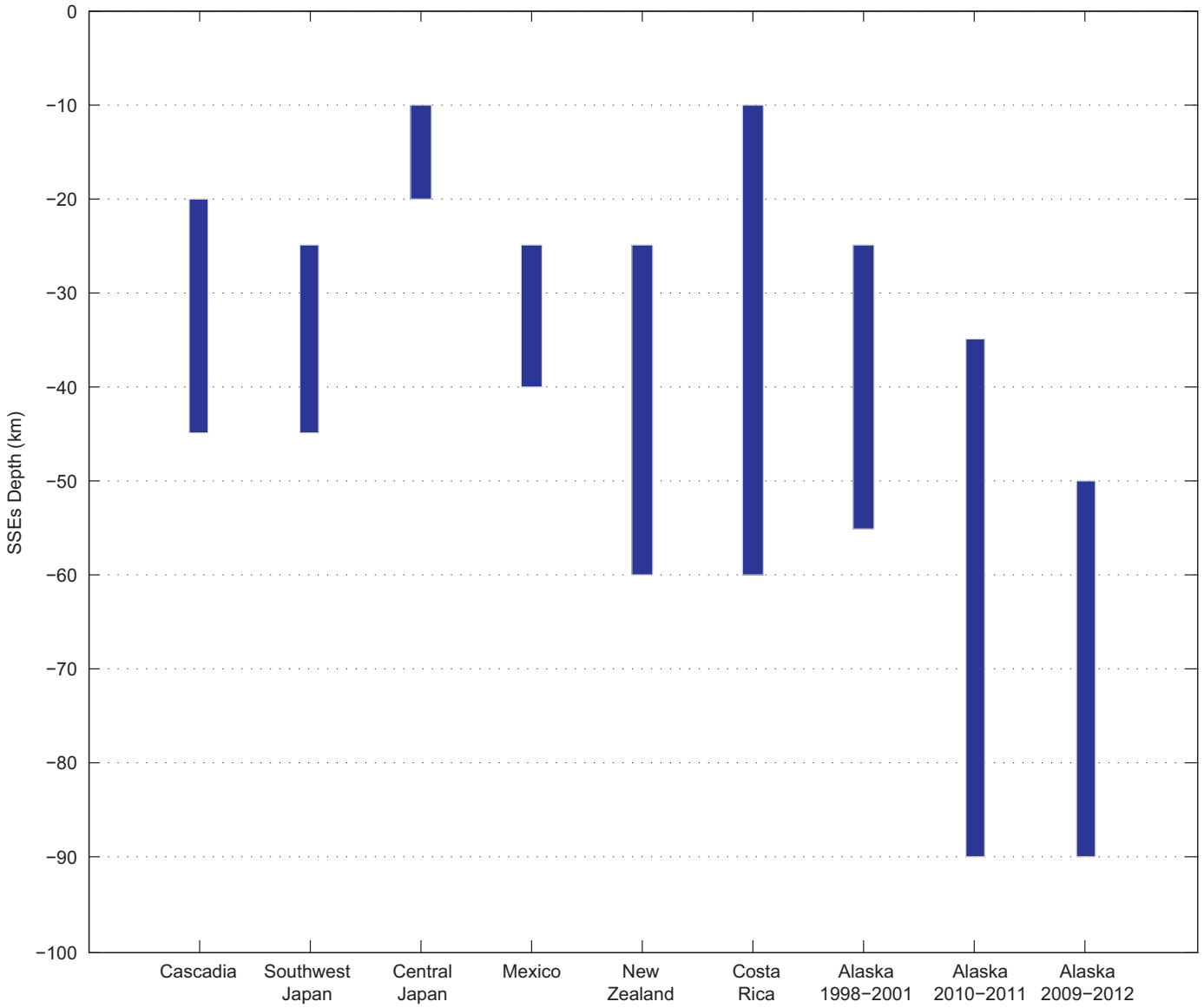

Fig. 8. Comparison of SSE depth ranges for events at several different subduction zones (Dragert et al., 2001; Hirose et al. 1999; Ozawa et al. 2003; Kostoglodov et al., 2003; Wallace and Beavan 2006; Jiang et al., 2012; Ohta et al., 2006; Wei et al., 2012; Schwartz and Rokosky, 2007). The Alaska events have occurred at generally greater depth than at the other subduction zones.

Acknowledgments

The authors are grateful to Donald Argus for helpful discussions and suggestions. We thank the Slab1.0 team for sharing their subduction slab geometry data. We appreciate two anonymous reviews for comments that significantly improve the manuscripts. This work was supported by NSF Grant EAR-1215933 to JTF, and a Global Change Student Grant to YF.

Appendix A. Auxiliary material

Supplementary data associated with this article can be found in the online version at http://dx.doi.org/10.1016/j.epsl.2013.05.049.

References

Argus, D.F., Gordon, R.G., Heflin, M.B., Ma, C., Eanes, R.J., Willis, P., Peltier, W.R., Owen, S.E., 2010. The angular velocities of the plates and the velocity of Earth's center from space geodesy. Geophys. J. Int. 180, 913–960, http://dx.doi.org/10.1111/j.1365-246X.2009.04463.x.

Brown, L.D., Reilinger, R.E., Holdahl, S.R., Balazs, E.I., 1977. Postseismic crustal uplift near Anchorage, Alaska. J. Geophys. Res. 82 (23), 3369–3378, http://dx.doi.org/10.1029/JB082i023p03369.

Cohen, S.C., Freymueller, J.T., 2004. Crustal deformation in Southcentral Alaska: the 1964 Prince William sound earthquake subduction zone. Adv. Geophys. 47, 1–63.

Dragert, H., Wang, K., James, T.S., 2001. A silent slip event on the deeper Cascadia subduction interface. Science 292, 1525–1528.

Freymueller, J.T., Cohen, S.C., Fletcher, H.J., 2000. Spatial variations in present-day deformation, kenai Peninsula, Alaska, and their implications. J. Geophys. Res. 105, 8079–8101.

Freymueller, J.T., Woodard, H., Cohen, S., Cross, R., Elliott, J., Larsen, C., Hreinsdottir, S., Zweck, C., 2008. Active deformation processes in Alaska, based on 15 years of GPS measurements, in active tectonics and seismic potential of Alaska. In: Freymueller, J.T., et al. (Eds.), Geophysical Monograph Serics, 179. AGU, Washington, DC, pp. 1–42, http://dx.doi.org/10.1029/179GM02.

Fu, Y., Freymueller, J.T., 2012. Seasonal and long-term vertical deformation in the Nepal Himalaya constrained by GPS and GRACE measurements. J. Geophys. Res. 117, B03407, http://dx.doi.org/10.1029/2011JB008925.

Fu, Y., Freymueller, J.T., van Dam, T., 2012a. The effect of using inconsistent ocean tidal loading models on GPS coordinate solutions. J. Geod. 86 (6), 409–421, http://dx.doi.org/10.1007/s00190-011-0528-1.

Fu, Y., Freymueller, J.T., Jensen, T., 2012b. Seasonal hydrological loading in southern Alaska observed by GPS and GRACE. Geophys. Res. Lett. 39, L15310, http://dx.doi.org/10.1029/2012GL052453.

Hayes, G.P., Wald, D.J., Johnson, R.L., 2012. Slab1.0: a three-dimensional model of global subduction interface geometries. J. Geophys. Res. 117, B01302, http://dx.doi.org/10.1029/2011JB008524.

Hirose, H., Hirahara, K., Kimata, F., Fujii, N., Miyazaki, S., 1999. A slow thrust slip event following the two 1996 Hyuganada earthquakes beneath the Bungo Channel, southwest Japan. Geophys. Res. Lett. 26, 3237–3240.

Hreinsdóttir, S., Freymueller, J.T., Bürgmann, R., Mitchell, J., 2006. Coseismic deformation of the 2002 Denali Fault earth-quake: insights from GPS measurements. J. Geophys. Res. 111, B03308, http://dx.doi.org/10.1029/2005JB003676.

Jiang, Y., Wdowinski, S., Dixon, T.H., Hackl, M., Protti, M., Gonzalez, V., 2012. Slow slip events in Costa Rica detected by continuous GPS observations, 2002–2011. Geochem. Geophys. Geosyst. 13, Q04006, http://dx.doi.org/10.1029/2012GC004058.

Kostoglodov, V., Singh, S.K., Santiago, J.A., Franco, S.I., Larson, K.M., Lowry, A.R., Bilham, R., 2003. A large silent earth-quake in the Guerrero seismic gap, Mexico. Geophys. Res. Lett. 30 (15), 1807, http://dx.doi.org/10.1029/2003GL017219.

Ohta, Y., Freymueller, J., Hreinsdottir, S., Suito, H., 2006. A large slow Slip event and the depth of the seismogenic zone in the south central Alaska subduction zone. Earth Planet. Sci. Lett. 247 (1–2), 108–116, http://dx.doi.org/10.1016/j.epsl.2006.05.013.

Okada, Y., 1985. Surface deformation due to shear and tensile faults in a halfspace. Bull. Seismol. Soc. Am. 75 (4), 1135–1154.

Ozawa, S., Murakami, M., Tada, T., 2001. Time-dependent inversion study of the slow thrust event in the Nankai Trough subduction zone, southwestern Japan. J. Geophys. Res. 106, 787–802.

Ozawa, S., Miyazaki, S., Hatanaka, Y., Imakiire, T., Kaidzu, M., Murakami, M., 2003. Characteristic silent earthquakes in the eastern part of the Boso Peninsula, central Japan. Geophys. Res. Lett. 30 (6), 1283, http://dx.doi.org/10.1029/2002GL016665.

Peterson, C.L., Christensen, D.H., 2009. Possible relationship between nonvolcanic tremor and the 1998–2001 slow slip event, south central Alaska. J. Geophys. Res. 114, B06302, http://dx.doi.org/10.1029/2008JB006096.

Rogers, G., Dragert, H., 2003. Episodic tremor and slip on the Casca-dia subduction zone: the chatter of silent slip. Science 300, 1942–1943, http://dx.doi.org/10.1126/science.1084783.

Savage, J.C., 1983. A dislocation model of strain accumulation and release at a subduction zone. J. Geophys. Res. 88, 4984–4996.

Schwartz, S.Y., Rokosky, J.M., 2007. Slow slip events and seismic tremor at circum-Pacific subduction zones. Rev. Geophys. 45, RG3004, http://dx.doi.org/10.1029/2006RG000208.

Suito, H., Freymueller, J.T., 2009. A viscoelastic and afterslip postseismic deformation model for the 1964 Alaska earthquake. J. Geophys. Res. , http://dx.doi.org/10.1029/ 2008JB005954.

Wallace, L.M., Beavan, J., 2006. A large slow slip event on the central Hikurangi subduction interface beneath the Manawatu region, North Island, New Zealand. Geophys. Res. Lett. 33, L11301, http://dx.doi.org/10.1029/2006GL026009.

Wang, K., Wells, R., Mazzotti, S., Hyndman, R.D., Sagiya, T., 2003. A revised dislocation model of interseismic deformation of the Cascadia subduction zone. J. Geophys. Res. 108 (B1), 2026, http://dx.doi.org/10.1029/2001JB001227.

Wei, M., McGuire, J.J., Richardson, E., 2012. A slow slip event in the south central Alaska Subduction Zone and related seismicity anomaly. Geophys. Res. Lett. 39, L15309, http://dx.doi.org/10.1029/2012GL052351.

Yamamoto, E., Matsumura, S., Ohkubo, T., 2005. A slow slip event in the Tokai area detected by tilt and seismic observation and its possible recurrence. Earth Planets Space 57, 917–923.